IGRF Submission Report

Naomi Shakespeare-Rees[1], Philip W. Livermore[1], Christopher J. Davies[1], Hannah Rogers[2, 3], William J. Brown[4], Ciaran D. Beggan[4], and Christopher. C. Finlay[5]

[1]School of Earth and Environment, University of Leeds, UK
[2]ISTerre, Uni. Grenoble Alpes, France
[3]Centre National d'Etudes Spatiales, France
[4]British Geological Survey, Edinburgh, UK
[4]DTU Space, Technical University of Denmark, Denmark

October 14, 2024

1 Overview

This report details the methodology behind the University of Leeds SV prediction candidate for 2025-2030. The main novel feature of our method is that the flow is built locally, over 72 latitude/longitude boxes over the CMB surface, using Physics Informed Neural Networks. Each PINN has weights that are trained through the frozen-flux equation, in order to reproduce the given SV structure from the given main field. The SV prediction candidate was calculated in four steps:

1. We assume frozen-flux (no magnetic diffusion) with a steady flow during 2025-2030.
2. We calculate our (steady) snapshot of the flow for epochs 2024.0 The flow in each box was trained using the main field and SV from CHAOS-7.18 for the same epoch, using 5 different (randomised) starting initialisations for the network weights. For each box, the initialisation with the lowest SV residual between the calculated SV and the SV from CHAOS-7.18 is chosen, and these boxes are then stitched together to make a global flow. Each box overlaps with its neighbours in order to eliminate any edge-effects.
3. We evolve the main field using SV calculated via the frozen-flux equation in five yearly steps from 2025 to 2030. Our starting configuration, the main field in 2025, is formed from a linear extrapolation at degree 8, using the average main field in epochs 2023.0 and 2024.0, using CHAOS-7.18.
4. We take the average of the five predictions of SV, truncated at degree 8, for the IGRF SV prediction.

2 Methodology

The methodology used for this submission is a novel method of discovering flows at the CMB locally, based on Physics Informed Neural Networks (PINNs).

2.1 Data

To produce the global flows needed for the global SV prediction, a mosaic of regional flows were constructed, spanning a latitude space of within 6° of the geographic pole. The surface of the core mantle boundary, at a radius of 3485km, is carved up into 56 boxes spanning 20° by 45° in latitude/longitude, and 16 boxes spanning 15° by 45° for the boxes closest to the poles. Each box is then extended by 5° in each direction, overlapping with neighbouring boxes. While the flow is calculated for the whole box, we keep only the flow within the original boundaries. This minimises edge effects in the flow construction. Training data for the PINNs are generated from the radial components of the Main Field and the Secular Variation at grid points at a density of 1 point per degree, calculated either at 2023.0 or 2024.0 from the CHAOS-7.18 model (Finlay et al. 2020). The positions of the boxes, as well as the Secular Variation from CHAOS 7.18 in 2024.0, are shown in Figure 1. All training data is truncated at spherical harmonic degree 8. After training, the border of 5° is removed, shown in white on Figure 2, and then the boxes are 'stitched' together.

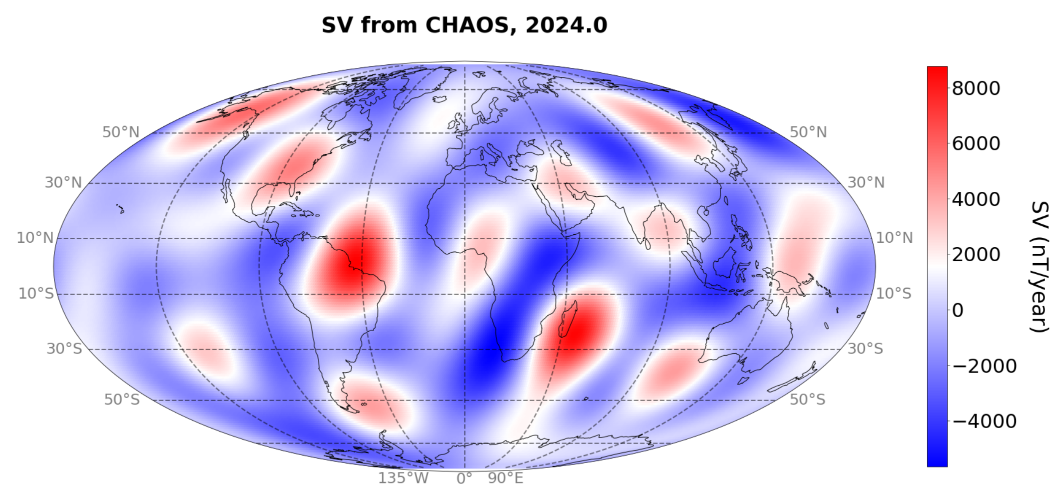

Figure 1: Box positions with SV from CHAOS-7.18 (epoch 2024.0), after the 5° border is removed. (Finlay et al. 2020), with continents shown for reference.

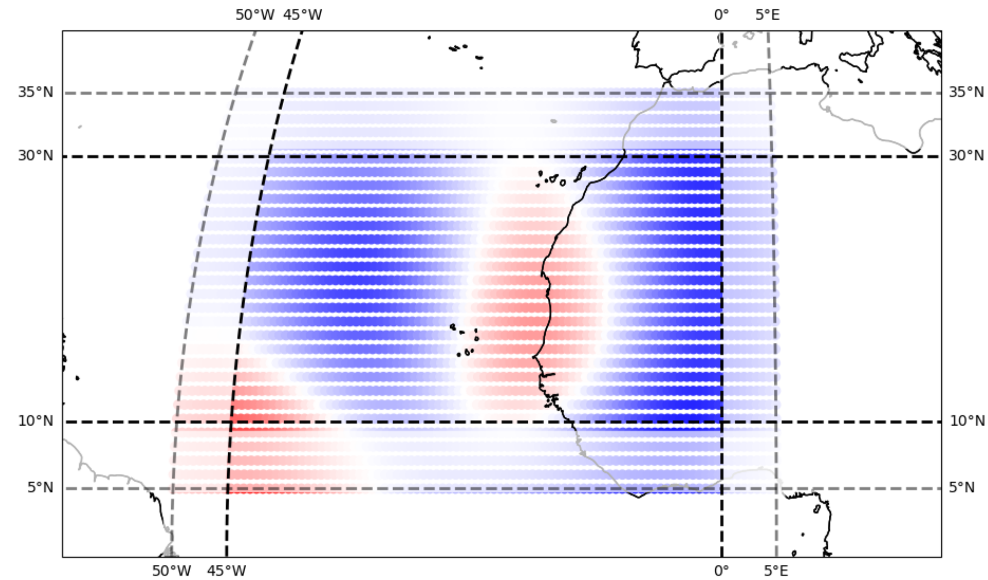

Figure 2: Example of a box used for inversion, the border removed after training is shown in white. SV at $l = 13$, with the same colour bar as in Figure 1, shown for reference.

2.2 Physics-Informed Neural Networks (PINNs)

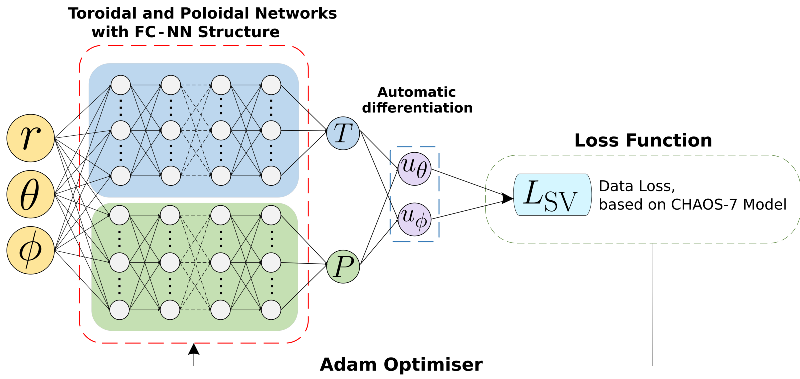

Figure 3: Schematic of PINN. r, θ, ϕ are the spherical coordinates, T and P the toroidal and poloidal scalars, and u_θ and u_ϕ the horizontal flows.

In spherical coordinates, we write the flow as

$$\mathbf{u} = \nabla \times T(\theta, \phi)\mathbf{r} + \nabla_H (rP(\theta, \phi)) \tag{1}$$

so that the expressions for the horizontal toroidal and poloidal flows can be written, respectively, (Holme 2007),

$$\boldsymbol{u}_T = \left(\frac{1}{\sin\theta} \frac{\partial T}{\partial \phi}, -\frac{\partial T}{\partial \theta} \right), \tag{2}$$

$$\boldsymbol{u}_P = \left(\frac{\partial P}{\partial \theta}, \frac{1}{\sin\theta} \frac{\partial P}{\partial \phi} \right). \tag{3}$$

There are two unknowns in these equations: the Toroidal scalar T, and the Poloidal scalar P. The inversion methodology consists of two Fully Connected Neural Networks (FC-NNs) working in parallel: one to describe the toroidal scalar T and the other to describe the poloidal scalar P. Once these scalars are recovered, the flows are then output using equations 2 and 3. Each FC-NN has 10 layers of 150 units; we use a swish activation function used for the internal units (Ramachandran et al. 2017), and a linear activation function for the final output units. We train the networks using the optimisation method Adam (Kingma and Ba 2017), which updates both networks simultaneously. The size for the Toroidal and Poloidal networks were found through grid sampling, in which many different network sizes were tested and the one with the minimum SV residual was chosen.

The loss term in the PINNs used for this submission consists of the MSE (mean squared error) between the SV recreated by the PINN-based flows and the SV from the CHAOS-7 model:

$$L_{\mathrm{SV}} = \frac{1}{N} \sum_{\theta,\phi} \left[-\left(\frac{1}{r} \left(\frac{u_\phi}{\sin(\theta)} \frac{\partial B_r}{\partial \phi} + u_\theta \frac{\partial B_r}{\partial \theta} \right) + B_r (\nabla_H \cdot \boldsymbol{u}) \right) + \frac{\partial B_r}{\partial t}_{CHAOS} \right]^2. \tag{4}$$

Although the PINN methodology allows us to apply additional physics-based flow constraints, we chose not to do this and to present the simplest possible model approach. While we do not explicitly apply smoothing to the flows, there is smoothing inherent to the modelling approach, in that our choice of network size is the smallest network for which the solutions reliably converge, and our choice to overlap the boxes. It is apparent from the SV and flows that the PINNs do not generate arbitrarily rough flows, perhaps also due to the smoothing present in CHAOS-7.18. For each box, the corresponding model is trained for 5000 iterations to ensure that the model has converged, and is trained from 5 different starting configurations of the weights. Of these 5 models, that with the lowest SV residual is chosen to be the 'best model' for that regional box.

2.3 Recovered SV and flows in 2024

To illustrate the method at epoch 2024.0, we show the flow-predicted SV and SV residuals in Figure 4. The corresponding flows are shown in Figure 5, evaluated on the same grid used for training. The Root Mean Square Error between the recovered SV and CHAOS SV is 66 nT/year, and the maximum SV residual is 347 nT/year. At the epoch in which the PINN is trained, the recovered SV agrees well with the training SV.

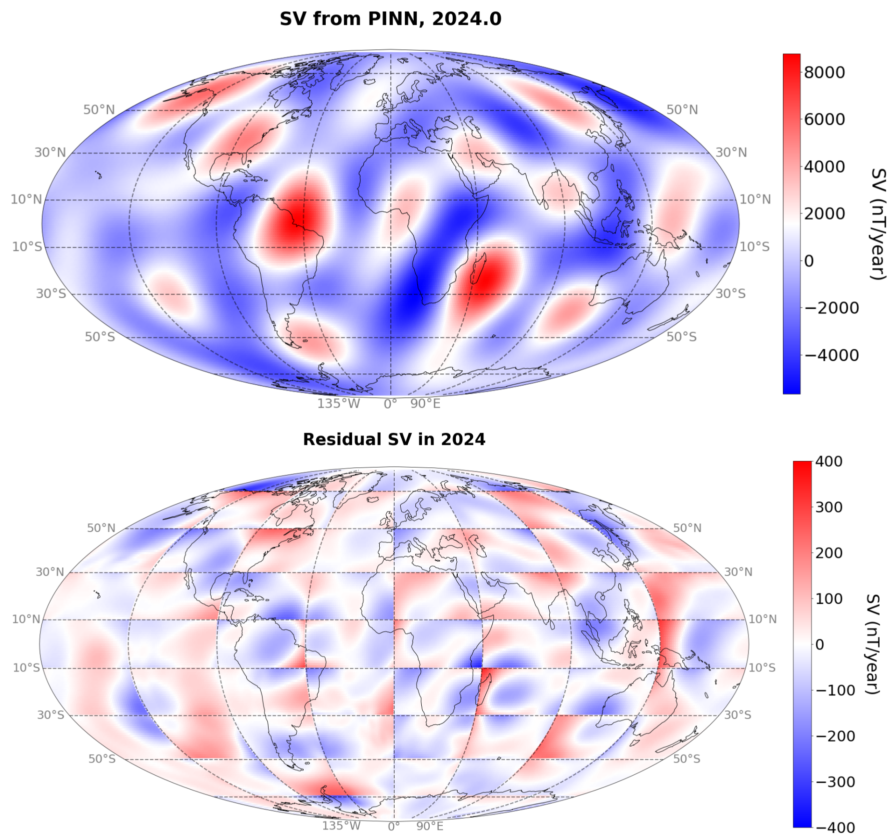

Figure 4: (Top) Recovered SV from PINN in 2024.0, evaluated on the grid described in Section 2.1. (Bottom) Residual between SV from CHAOS and recovered SV.

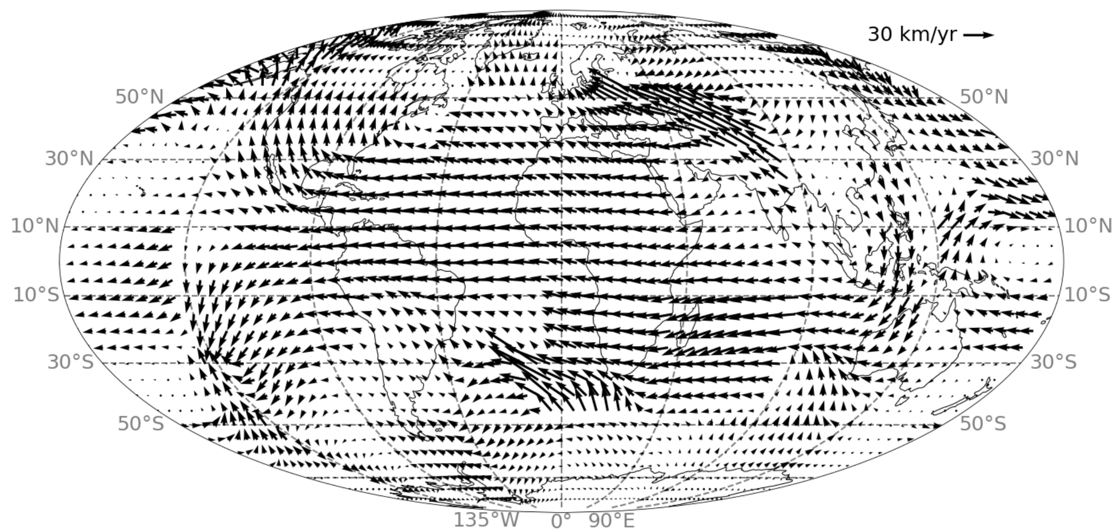

Figure 5: Recovered Flows in 2024.0, shown using streamlines. Colours show the longitudinal flow.

2.4 SV Prediction

Our SV prediction is based on evolving the frozen-flux induction equation from 2025 to 2030, for which we calculate the averaged SV.

We require an estimate of the main field in 2025, which is based on the main field in 2024 corrected by an averaged SV. We calculated an averaged SV from 2023 to 2024 - $\boldsymbol{SV}_{av}$ - by taking the mean of the SV on 1st January 2023 and 1st January 2024, at spherical harmonic degree 8. This average SV, multiplied by the time step Δt, is then added to the radial field in 2024 such that:

$$\boldsymbol{B}_{2025} = \boldsymbol{B}_{2024} + \boldsymbol{SV}_{av}\Delta t, \tag{5}$$

where Δt is 1 year. The flow in Figure 5 is assumed constant for the period of 2025-2030, No flow smoothing is used in this SV prediction. For each yearly time step t through this period, the main field was evolved using:

$$\boldsymbol{B}_{t+1} = \boldsymbol{B}_t + \boldsymbol{SV}_t = \boldsymbol{B}_t + \nabla \times (\boldsymbol{u} \times \boldsymbol{B}_t). \tag{6}$$

Numerically, we evaluate both the main field (degree-8) and flow on a Gauss-Legendre-Fourier Grid, taking spherical harmonic transforms to find the SV in terms of Gauss coefficients (to degree 8). We use a grid size capable of exactly resolving the required SV using a flow to degree 27. This is linearly interpolated up to the poles by transforming the coordinates such that there is no singularity at the poles. The SV updated at each step produced a prediction for the SV every year for the period 2025-2030, at degree 8. The mean of these models was then taken, and the Gauss coefficients for the resulting SV model were truncated to spherical harmonic degree 8 for submission to the IGRF. The prediction for $l = 8$ is shown in Figure 6. The spatial power spectrum at the CMB is shown in Figure 7, and the equivalent at the Earth's Surface shown in Figure 8.

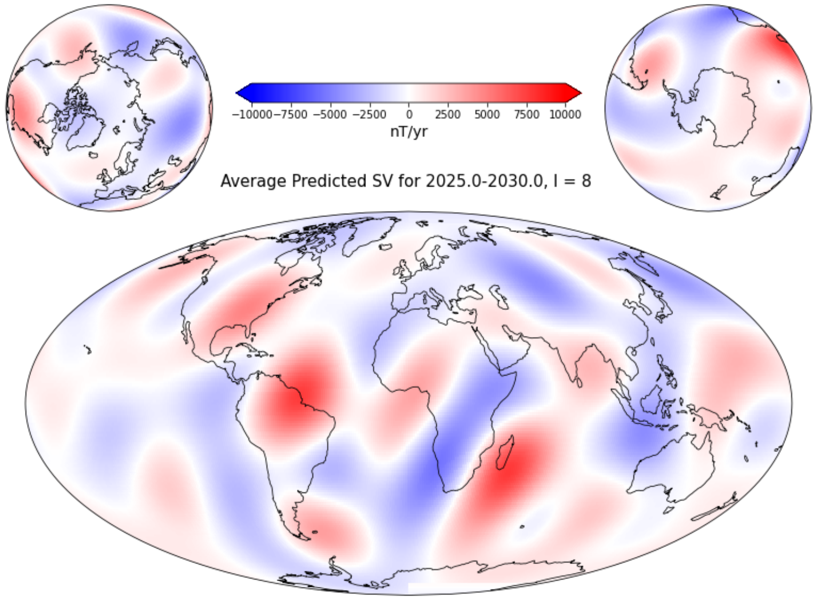

Figure 6: Predicted SV for 2025.0-2030.0 at degree 8.

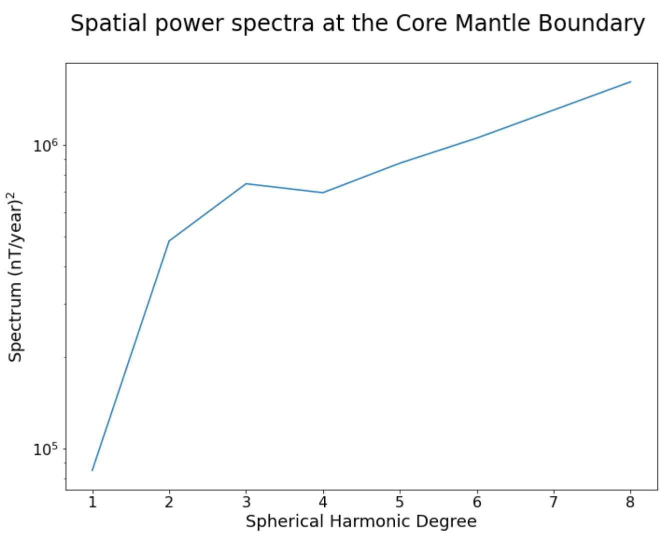

Figure 7: Spatial Power Spectra of the predicted SV at the Core Mantle Boundary, $r = 3485km$, plotted using ChaosMagPy (Kloss 2024).

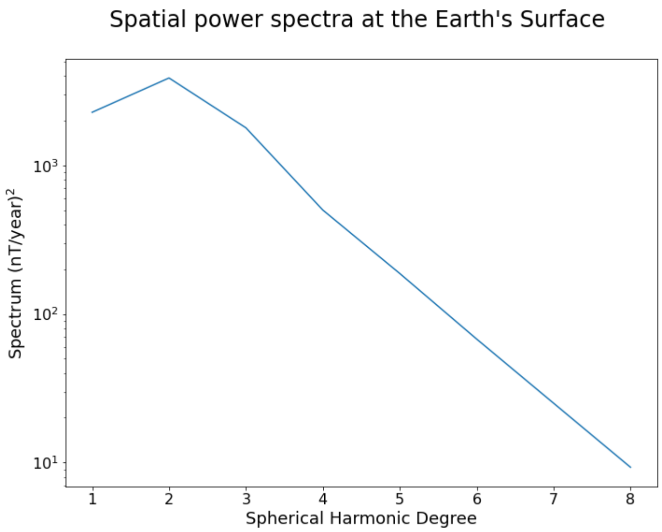

Figure 8: Spatial Power Spectra of the predicted SV at the Earth's Surface, $r = 6371km$, plotted using ChaosMagPy (Kloss 2024).

References

Finlay et al. (Oct. 2020). "The CHAOS-7 geomagnetic field model and observed changes in the South Atlantic Anomaly". In: 72, p. 156. ISSN: 1880-5981. DOI: 10.1186/s40623-020-01252-9.

Holme, R. (Jan. 2007). "8.04 - Large-Scale Flow in the Core". en. In: *Treatise on Geophysics*. Ed. by Gerald Schubert. Amsterdam: Elsevier, pp. 107–130. ISBN: 978-0-444-52748-6. DOI: 10.1016/B978-044452748-6.00127-9. URL: https://www.sciencedirect.com/science/article/pii/B9780444527486001279.

Kingma, Diederik P. and Jimmy Ba (Jan. 2017). "Adam: A Method for Stochastic Optimization". In: arXiv:1412.6980. arXiv:1412.6980 [cs]. DOI: 10.48550/arXiv.1412.6980. URL: http://arxiv.org/abs/1412.6980.

Kloss, Clemens (June 2024). *ancklo/ChaosMagPy: ChaosMagPy v0.14*. DOI: 10.5281/zenodo.12200898. URL: https://zenodo.org/records/12200898.

Ramachandran, Prajit, Barret Zoph, and Quoc V. Le (Oct. 2017). "Swish: a Self-Gated Activation Function". en. In: arXiv:1710.05941. arXiv:1710.05941 [cs]. URL: http://arxiv.org/abs/1710.05941.